Special Issue: Vesuvius monitoring and knowledge

Flood hazard of the Somma-Vesuvius region based on historical (19-20th century) and geomorphological data

Giuliana Alessio[1,*], Melania De Falco[2], Giuseppe Di Crescenzo[3], Rosa Nappi[1], Antonio Santo[3]

[1] *Istituto Nazionale di Geofisica e Vulcanologia, Sezione di Napoli, Osservatorio Vesuviano, Naples, Italy*

[2] *Università di Napoli "Federico II", Dipartimento di Scienze della Terra, dell'Ambiente e delle Risorse, Naples, Italy*

[3] *Università di Napoli "Federico II", Dipartimento di Ingegneria Civile, Edile ed Ambientale, Naples, Italy*

Article history
Received October 1, 2012; accepted June 25, 2013.
Subject classification:
Flood hazard, Geomorphological data, Somma-Vesuvius.

ABSTRACT

This paper presents a preliminary susceptibility map of the flood hazard for the Somma-Vesuvius volcanic district, worked out by means of multi-disciplinary historical, geological, geomorphological and rainfall data processing. It is well known that the Somma-Vesuvius volcano, due to its explosive volcanism and the dense urbanization of the surrounding area, with a population exceeding 650,000 is one of the most dangerous active volcanoes of the world. Although this area has been extensively studied from the volcanological point of view with regards to its volcanic hazard, there are currently not many detailed studies about its flood hazard factors, despite the fact that, in the last century, many intense rainfall events in this area have produced several floods that invaded the surrounding plains affecting towns and roads, and causing much damages and loss of lives. Accordingly, in this paper high-resolution DEM (5×5 m pixel) and detailed geomorphological maps of the whole area have been analyzed and processed in GIS environment, carrying out a comparative study of the present-day morphology and the morphology of the 1900's volcanic edifice, including changes of infrastructures and buildings throughout the last century. These results, together with historical chronicles data and the rainfall accurate data for all flood events, have been processed in this paper for highlighting the drainage basins areas of Somma-Vesuvius where the flood phenomena could be more probable in the future, working out a preliminary zoning map, also suggesting in which sectors interventions useful for mitigation of flood risk should be implemented.

1. Introduction

The Somma-Vesuvius volcanic district is located in the Campanian Plain, a structural depression formed along the southern Italy Tyrrhenian margin e.g. [Scandone et al. 1991] (Figure 1).

The volcanic complex is composed by the older caldera of Mt. Somma that contains the younger cone of Mt. Vesuvius. Volcanic activity dates back to about 25 ky [Cioni et al. 1999], with effusive eruptions and explosive Plinian and sub-Plinian eruptions, alternated to long-lasting quiescence periods [Scandone et al. 1993, Nazzaro 2001, Andronico and Cioni 2002]. The Mt. Vesuvius is an active, composite strato-volcano in a quiescent status since 1944; due to its explosive volcanism and the dense urbanization of the surrounding area with a population exceeding 650,000, this volcano is one of the most dangerous of the world, with population density of about 3000 inhabitants for square kilometer (Figure 1). Indeed, besides the volcanic hazard, additional conspicuous hazard is related to lahars phenomena: flows of unconsolidated debris and water that typically include fragments of volcanic origin, colluvium, and soil; the features of such lahars can range from debris flow to hyperconcentrated flow [Smith and Lowe 1991, Lirer et al. 2001]. The volcanic complex has been extensively studied from the volcanological point of view and regards the volcanic hazard [Cioni et al. 2008, Mastrolorenzo and Pappalardo 2010], but only a few scientific papers have focused on a different kind of hazard, like the flood hazard of the Somma-Vesuvius whole district [De Vita and Vallario 1996, Lirer et al. 2001]. Disastrous floods, reported in historical literature, have repeatedly affected the area causing much damages and loss of lives [Accardo et al. 1981, Catenacci 1992, Cosenza 1997]. The flood phenomena are described as rapid events, not forecasted, but rarely rockfalls or flow-type landslides [Davies and Mc Saveney 2011]. Particularly, the river basins of the main fluvial and torrential rods in the Somma-Vesuvius territory have been studied with regard to their geomorphological, vegetation, soil use and hydrologic parameters [Russo et al. 1995, Davoli et al. 2001, Di Crescenzo et al. 2008]. De Vita and Vallario [1996] have analyzed the specific features of the Cavallo channel, a riverbed located upstream of the Torre del Greco built-up area,

through a statistical-probabilistic analysis of the most intense precipitations, estimating return periods of few tens of years. Most recently, hazard and risk maps for local landslides and hydraulic phenomena have been compiled through the PAI (Piano di Assetto Idrogeologico. Autorità di Bacino del Sarno, http://www.autoritabacinosarno.it/default.asp; Piano di Assetto Idrogeologico. Autorità di Bacino Nord Occidentale della Campania, http://www.autoritabacinonordoccidentale.campania.it/default1.asp).

In this paper, in order to study the flood hazard for the Somma-Vesuvius volcanic area, a dedicated Geographic Information System (GIS) has been implemented, composed by four database, which provides: i) the capability for storing and managing large amounts of spatial data; ii) the detection of areas with specific conditions through the overlay of different thematic maps; iii) the prediction of the dynamics of natural phenomena through sophisticated use of mathematical operators or integrated numerical models. The operation of this GIS system has enabled us to process and generate many original informative layers, through image analysis, for assessment of hazard and risk posed by meteorological extreme events which may cause floods. The combined analysis of geological-geomorphological data, rainfall events catalogue and existing infrastructures has provided insights on the triggering mechanisms and on the susceptibility or probability of new future events in the area under study, and on their expected intensity as well. Moreover the strong changes of the exposed values (buildings and roads) in the last century have been evaluated for assessment of the impact of future extreme events on the environment [Pareschi et al. 2000, Nappi et al. 2008].

2. The GIS database

The GIS database implemented for our study is based on historical (19-20th century) and recent data assembled into the following complementary databases: (a) the database of geomorphological parameters; (b) the database of drainage networks; (c) the database of pluviometric events and historical record of floods; (d) the database of whole infrastructures including changes due to the strong urbanization of the area throughout the last century.

The analysis of these space-time series of data has been carried out using a high resolution DEM (5×5 m pixel), generated by the Triangulation Irregular Network (TIN) interpolation technique through ArcGIS ESRI Software using the numeric cartography CTPN (Carta Tecnica Provinciale Numerica) of Province of Naples, at scale 1:5000 [Vilardo et al. 2008]. The DEM (Figure 1) is referenced to UTM zone 33 with the WGS-84 ellipsoid.

At first, in this paper the existing early 1900 topographic maps have been retrieved in the Library of the Osservatorio Vesuviano, scanned and geo-referred

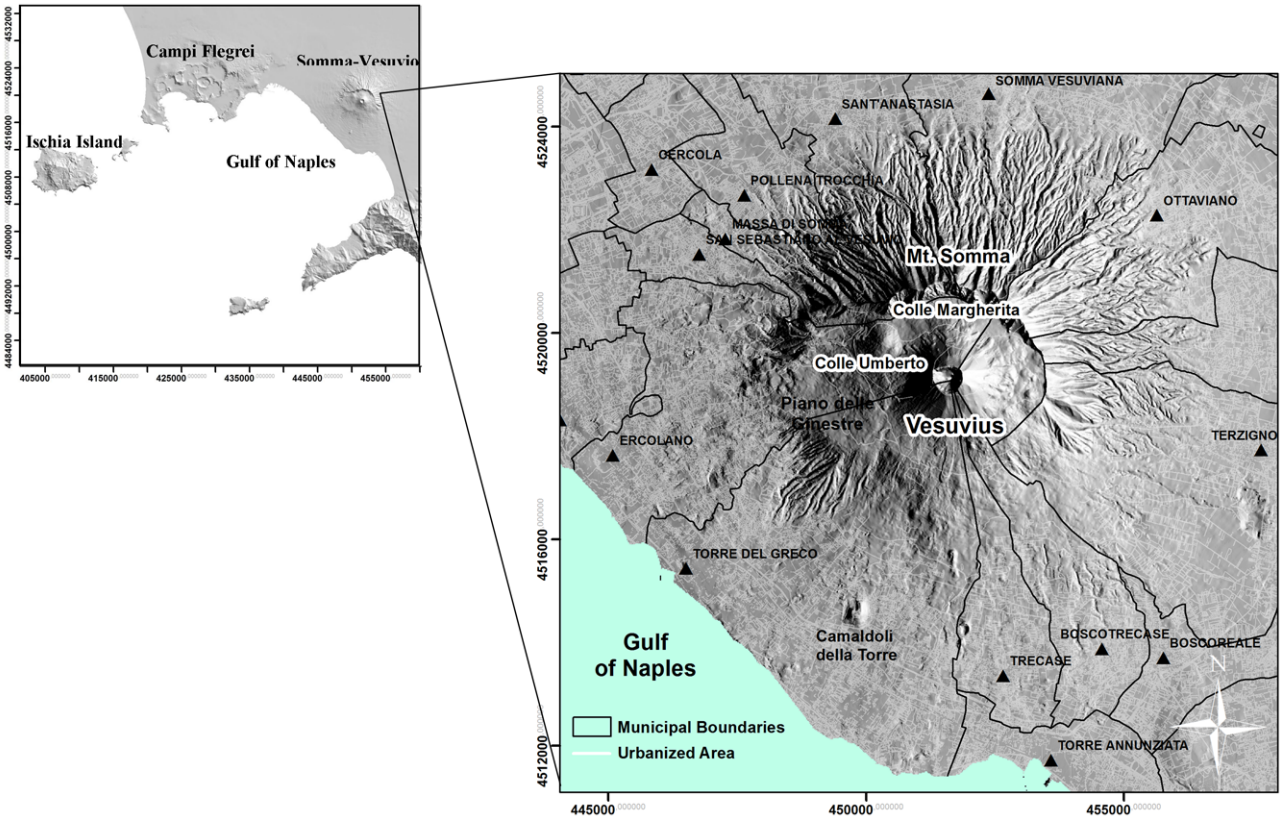

Figure 1. Location and shaded relief of the Somma-Vesuvius volcanic complex.

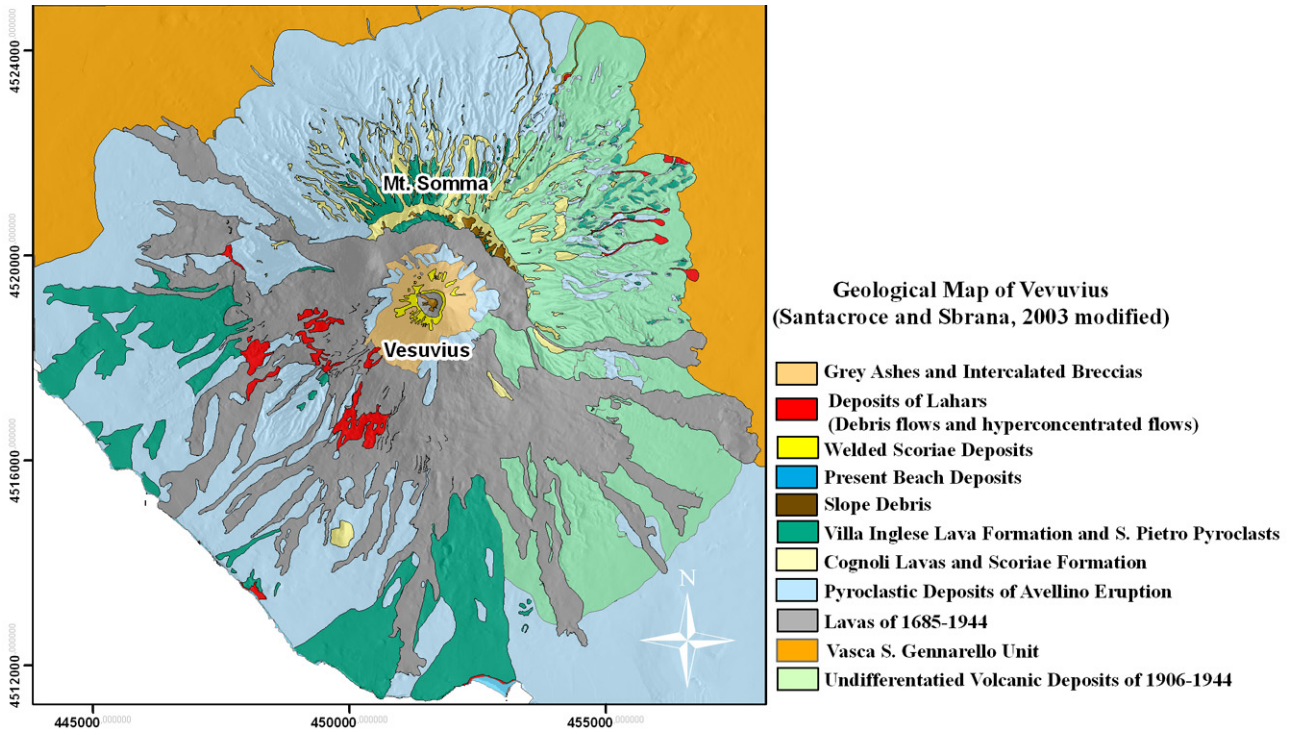

Figure 2. Geological Map of the Somma-Vesuvius volcanic complex (after Santacroce [1987], and Santacroce and Sbrana [2003], modified).

(UTM-WGS84) in order to compare the ancient urbanized areas with the corresponding areas of the last decades by means of the CTPN, 1998. The available historical data have pointed out the basins that have been mostly affected by alluvial events and, consequently, the geological and geomorphological parameters of such basins particularly prone to the alluvial events have been investigated.

From a geological point of view, the areas characterized by pyroclastic products coverage have been recognized, extracted from the Geological Map of Santacroce and Sbrana [2003] (Figure 2) and grouped in few main classes based on their permeability [Chirico et al. 2010]. The geomorphological parameters extracted from DEM have been estimated on the catchment basins of the volcanic system with a detailed temporal analysis.

Moreover, we have carried out a comprehensive examination and synthesis of the hydrogeological instability phenomena occurred in the Somma-Vesuvius volcanic area. Extensive historical data collection about local floods have been retrieved through archives and database online available [AVI and IFFI Project], municipal and scientific publications. As regards the alluvial phenomena, for each alluvial event the daily and, whenever possible, hourly pluviometric data have been collected and stored up.

Finally, these space-time series of data, integrated with updated territorial information and compared with different thematic maps, have been used to elaborate a preliminary map of susceptibility to floods phenomena for the Somma-Vesuvius volcanic district.

2.1. The database of geomorphological parameters

The geomorphological database includes: the high resolution DEM (5×5 m pixel) in grid format, as the basis for our calculation; the Geological Map of Santacroce and Sbrana [2003] (Figure 2) and the Geomorphological Map of Ventura et al. [2005] (Figure 3), in vector format. The Topographical maps in raster format of the 1906, 1950 and 2004 years, at different scale (1:25.000, 1:10.000, 1:5000), scanned and geo-referred (UTM-WGS84), and the thematic maps derived from DEM [Karatson et al. 2010] such as the Slope map (Figure 4a), the Shaded relief (Figure 1), the TPI (Topographic Position Index) map (Figure 4b) and the map of the catchments basins in Figure 5, represent the new data.

The Somma-Vesuvius Map of Santacroce and Sbrana [2003] is the geologic map used for recognizing the areas with pyroclastic products coverage and for grouping them in few main classes based on their permeability (Figure 2). Each geologic formation has been vectorialized and represented with different colours respect to the original ones since we have grouped formations with the same lithologic characteristics. The Mt. Somma products mainly consist of lava and scoriae deposits, whereas products from highly explosive eruptions (i.e. pumice blankets, pumice flows, block and ash flows) are very limited. Five sub-Plinian eruptions occurred between 16,1 ka and A.D. 1631 [Andronico et al. 1996a, 1996b]; the deposits of these eruptions mainly consist of pyroclastic fall, flow and surge deposits, whereas gravity-driven volcaniclastic flows (hyperconcentrated flows, debris flows) crop out extensively on

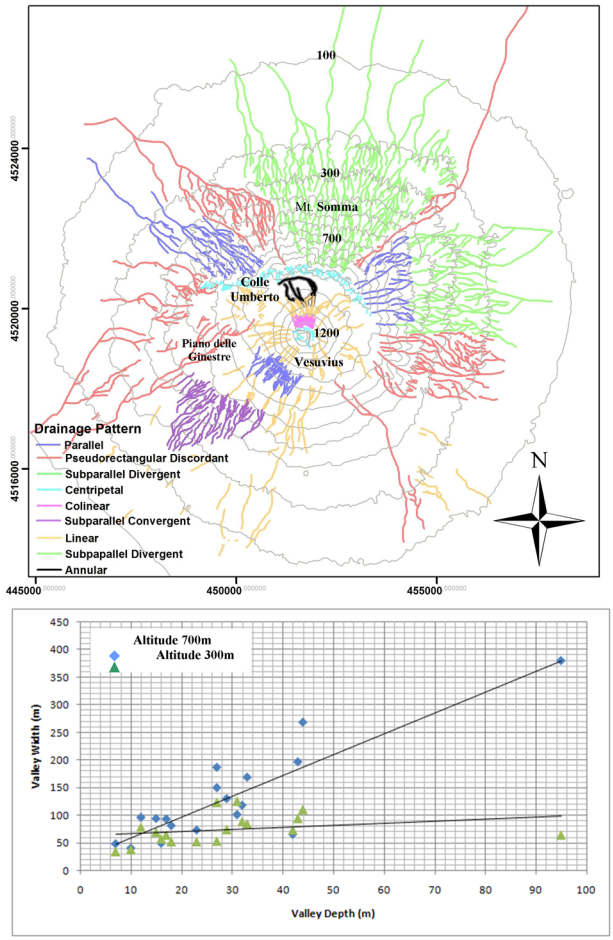

Figure 3. a) Drainage Pattern map of Somma-Vesuvius from Ventura et al. [2005], modified; b) relationship between width and depth of the valleys at 700m and 300m of elevation.

the northern and eastern flanks of the volcano (Figure 2). Minor outcrops occur on the southern and western flanks, where the deposits mainly consist of pyroclastic flows (Figure 2). Lava flows of the 1637-1944 period filled the caldera depression and extensively cover the southern and western flanks of the volcano. The semi-persistent activity of this period is also responsible for the growth of the present-day Vesuvius cone. Deposits of hot avalanches related to the A.D. 1944 eruption occur all around the base of the Vesuvius cone (Figure 2).

The Drainage map (Figure 3) extracted from Ventura et al. [2005] is the map representing the current drainage elements. The comparison with the past drainage conditions, extracted from the existing early 1900 Topographical maps, has been essential in order to deduce the different conditions influencing the floods hazard.

Despite the absence of any permanent stream, the Somma-Vesuvius drainage network is well developed on the NW, N, E and SW flanks of Mt. Somma and on the N and SW sectors of the Vesuvius crater (Figure 3). Different drainage patterns can be recognized in detail [Schumm 1977, Ollier 1991].

Pseudo-rectangular pattern occurs in the NW, NE, SE and W sectors. In the N and E sectors, the drainages are arranged in a subparallel divergent pattern. The drainage configuration in the northeastern sector of the volcano, which is mainly pseudo-rectangular, shows a divergent component due to the presence of an evident NE-SW elongated ridge that extends from the caldera rim to the ring-plain. Parallel drainage develops only in the upper zones of the NW and E flanks of Mt. Somma, where the streams follow NW-SE and E-W directions, respectively; a well developed NW-SE to WNW-ESE elongated valley (Fosso della Vetrana) sep-

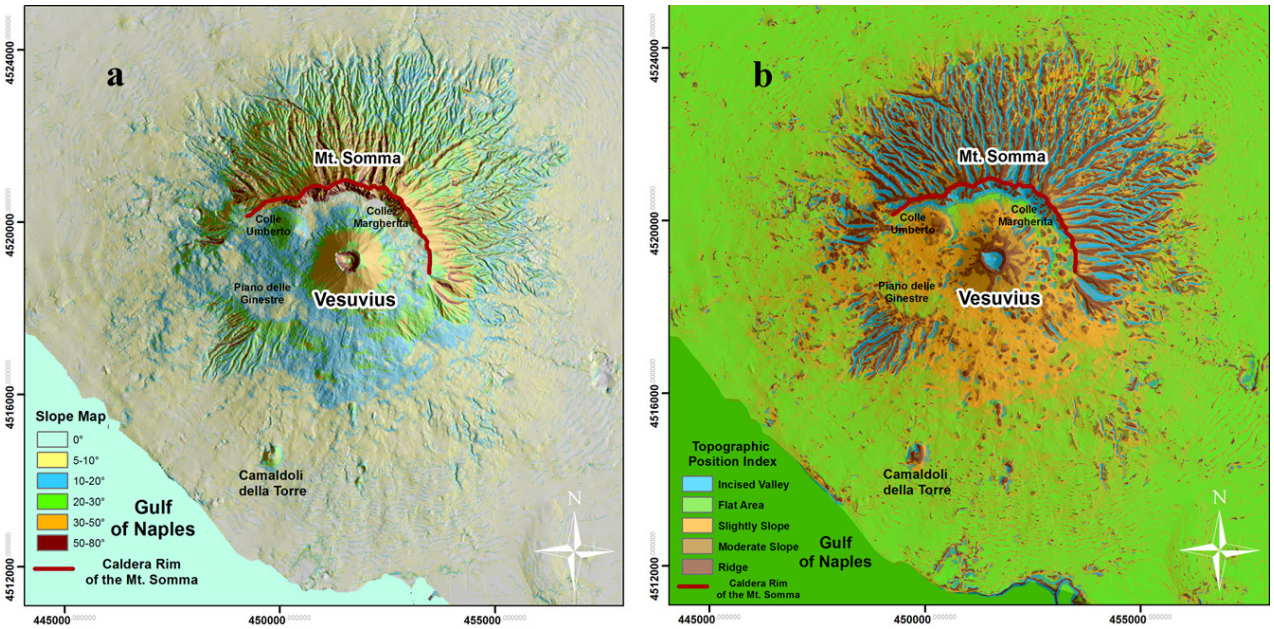

Figure 4. a) Terrain Slope map extracted from DEM (5×5 m pixel); b) Landforms classification map: the different colours represent the slope areal distribution (*slope position*) extracted from the Topographic Position Index (*TPI*) [Jenness and Tagil 2008, Chirico et al. 2010].

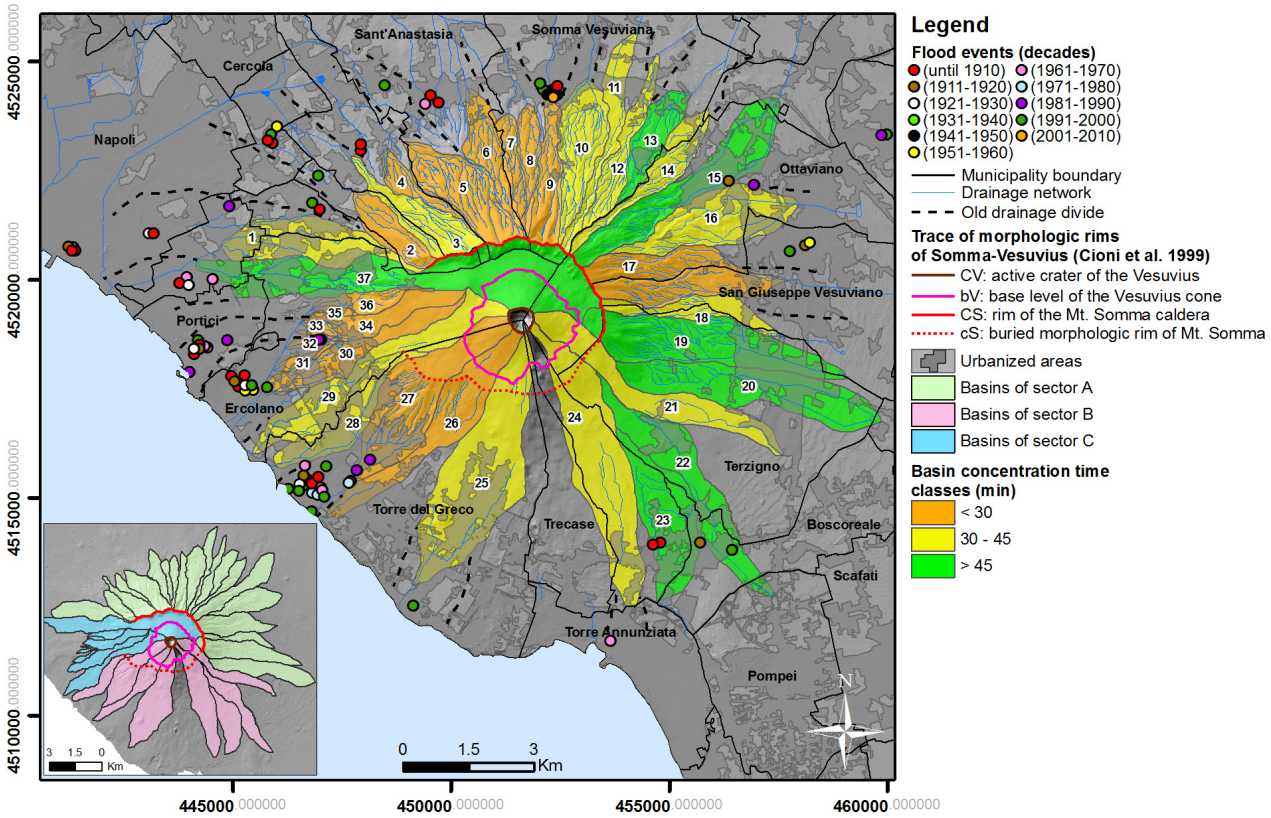

Figure 5. Catchments basins map of the Somma-Vesuvius complex, classified according to three concentration times classes (in minutes), the flood events location and the old drainage divides retrieval in the piedmont area and in the plain.

arates the northwestern flank of Mt. Somma from the northern one (Figure 3).

Inside the caldera, different drainage patterns can be recognized. Centripetal drainage characterizes the south-facing scarp of the caldera rim as well as the inner side of the Vesuvius crater.

Immature stage drainage characterizes the outer flanks of the Vesuvius cone and the Colle Umberto relief, where the drainage is arranged in a radial pattern (Figure 3). Drainage pattern that extends from the Vesuvius cone and laterally bounds the Colle Margherita relief on the northern slope of Vesuvius, defines an annular pattern. On the top of the NE sector of the Vesuvius cone, gullies organized in a collinear pattern affect the A.D. 1944 eruption pyroclastic products.

The analysis of the drainage pattern remarks that the drainage of Mt. Somma caldera, especially in the northern side, is mature and not influenced by lithology, while that of Vesuvius is immature and dissected by rill erosion [Cotton 1944], but there are some exceptions. The southwestern sector of the volcano is influenced by the geological composition of its deposits, particularly where the lava outcropping does not allow streams erosion, with the exception of Piano delle Ginestre.

The lack of significant differences between width and depth of the valleys at 700 m and 300 m of elevation (Figure 3b), which represent the hills on the bottom and on the top of volcanic edifices respectively, support the thesis that the drainage not influenced by lithology.

The thematic maps of Terrain Slope, Topographic Position Index (TPI) [Jenness and Tagil 2008] (Figure 4a,b) and the map of basins derived from the high resolution DEM of Somma-Vesuvius [Vilardo et al. 2008] have allowed us to understand influence of geomorphological features on floods events development. In detail the TPI has been useful for determining shape of relief in order to characterize behavior of rivers.

The Somma-Vesuvius consists of an asymmetric, truncated cone-like structure (Mt. Somma volcano, 1131 m a.s.l.) characterized by a summit, slightly E-W elongated flat area (Mt. Somma caldera area, slope between 5-15°; Figure 4a). A south-facing steep scarp with slope of about 80° bound the area, which correspond to the caldera rim, arc-shaped in the north and eastern sectors. The scarps on the incised valleys of the northern, south-eastern and rarely south-western flank of the Somma-Vesuvius complex (Figure 4b) are characterized by slope of about 40-80°. Moreover, the summit portion of the Vesuvius cone (1281 m a.s.l) showes slope values >35°.

The southern and western sector of the piedmont area (slope between 10-20°) is bounded by two arc-shaped convex breaks in slope. An arc-shaped convex break in slope extends from this sector of the volcano to the NW Somma outer flank. An additional arc-shaped

convex break in slope occurs inside the flat area. Minor sub-circular positive forms occur inside the caldera.

On the flanks of the cone several convex breaks in slope occur, whereas its base is characterized by positive, slightly elongated, poly- to uni-lobate forms with almost flat tops and steep borders (Figure 4b). On the NW of the cone, two positive forms NW-SE elongated (Colle Umberto) and sub circular (Colle Margherita) occur (Figure 4b).

The Somma-Vesuvius is surrounded to the N, NW, E and SE by a semi-circular area characterized by gentler slope (<10°) that represents the apron, and by a flat area (slope <5°) that sets the limits of the alluvial plain s.s.(Figure 3a). These two areas are lacking in the western and southwestern sectors due to the presence of an almost rectilinear, NW-SE striking coastline.

Valleys and ridges extend in a radial pattern from the caldera rim to the ring plain on the northern, eastern and part of the western Mt. Somma flanks, whereas significant incisions and ridges are absent in the southern sector (Figure 4b). A NE-SW elongated major ridge, which is also evidenced by a main NE-SW striking rectilinear valley and by divergent pattern of second-order drainages, extends from the NE rim of the caldera to the ring plain.

2.2. The database of drainage networks

The main catchment basins of the Somma-Vesuvius have been extracted from a large scale topographical map (Regional Technical Map of Campania region, scale 1:5000, 2004) and digitized on the shaded relief map of Figure 5.

A total number of 37 catchment basins have been recognized through the "Arc Hydro Tools" application in GIS environment; their existence has also been verified through geomorphological approach, since the whole area shows high hydrographical complexity due to volcanic and antropogenic activity. Particularly, in the piedmont and plain sectors of the area the current rivers pattern has been compared with the trend shown by the same rivers in 1906 (Figure 5), reconstructed through older topographical maps. Such analysis has allowed us to identify the main run-off areas recognized through the main divides which are not currently evident since wholly concealed by the urbanized areas. The position of the divides and of the run-off areas points out that some of the basins identified on a recent topographical maps showed the same ending point into the plain (for example 30-31-32; 33-34; 35-36 etc). Such approach has allowed us to assign more correctly the retrieved alluvial events to the catchment basins in which they occurred (Table 1).

The main geomorphological and planimetric parameters of such basins have been calculated and quoted in Table 1. These parameters show up the morphologic diversity between the northern and southern sector of the Somma-Vesuvius complex. In general, from the basins analysis it has been recognized that the basins with greater areal extension and greater relief energy are mainly located in the southern and southern-western sector. Particularly, the areal extensions are of 3-5 km^2 for basins nos. 26, 27 and 29, and greater than 5 km^2 for basins nos. 24, 25 and 37. Also in the eastern sector the basins no. 15 up to no. 23 exceed 5 km^2. As regards the average slope, the basins with greater slope (>15%) are no. 2 up to no. 10, and are located in the northern sector. Finally, as regards the average slope of the main fluvial roads, the southern-western and northern basins are characterized by the greatest slope values (> 5%).

Moreover, the northern basins show well defined watersheds with maximum altitudes between 800 and 1250 meters a.s.l., average slope values between 15° and 20°, and relief energy between 500 and 1000 meters a.s.l. On the contrary, the southern basins lack of well defined watersheds, show maximum altitudes between 250 and 1250 meters a.s.l., average slope values between 10° and 12°, and relief energy between 100 and 1200 meters a.s.l.

Such variations are also confirmed by some morphological elements due to the volcanological evolution of the Somma-Vesuvius complex [Cioni et al. 1999], like the crater rim position of the Mt. Somma that is well delineated to the north, but hardly recognizable to the south; moreover the actual location and the boundary of the Vesuvius cone, detectable through the slope breakdown existent on its baseline (line bV in Figure 5). These elements have allowed us to distinguish three different sectors A, B and C in Figure 5. The sector A includes the basins B1 up to B20 that are situated to the north of Mt. Somma (line CS in Figure 5). The sector B is located to the south of the volcanic complex and includes the basins B21 up to B28 that are situated in the southern mountainside of the Vesuvius (uphill of the bV line) and of the Mt. Somma (to the south of the cS line). Finally, the sector C is located to the west of the Somma-Vesuvius complex where the cS line is not clearly discernible since it has been probably obliterated by the various paroxisms of Vesuvius activity [Cioni et al. 1999].

The above mentioned morphological variations are also clearly recognizable both through the hypsographic curves shown in Figure 6 and in some typical topographical profiles carried out in the three sectors that have been identified in this paper, and shown in Figure 7.

Number of basin	ne (nep)	A (km^2)	BMS (°)	BMe (m a.s.l.)	Bme (m a.s.l.)	BR (m)	La (km)	S (m/m)	TL (km)	DD (km/km^2)	Tc (h)	Qs (m^3/s)
B1	5 (5-B1, B2)	3.1	6.9	607	62	545	4.1	0.029	6.7	2.2	0.76	3.6
B2	1 (5-B1,B2) (4-B2, B3)	1.4	18.1	715	185	530	2.4	0.073	6.4	4.6	0.35	2.3
B3	1 (4-B2, B3)	2.0	23.5	1024	148	876	3.1	0.039	17.3	8.6	0.56	2.8
B4	1 (1-B4, B5)	0.9	18.7	829	163	666	2.8	0.097	10.1	11.6	0.36	1.4
B5	1 (1-B4, B5)	2.8	20	1099	169	930	3.3	0.090	34.8	12.5	0.42	4.4
B6	3	1.7	19.2	1026	149	877	3.1	0.083	17.4	10.2	0.42	2.6
B7		0.7	22.5	900	191	709	2.5	0.096	7.1	9.6	0.33	1.3
B8		1.0	21.6	1116	179	936	2.3	0.070	9.7	9.7	0.35	1.7
B9	7	1.7	25.2	1129	188	941	3.7	0.110	13.2	7.8	0.42	2.7
B10		2.6	15.4	1050	145	905	4.4	0.084	22.4	8.6	0.54	3.6
B11		1.7	2.7	1105	100	1005	5.7	0.076	6.1	3.7	0.68	2.1
B12		1.6	14.5	811	116	695	4.6	0.046	11.6	7.3	0.70	1.9
B13		1.6	10.9	577	128	449	3.6	0.042	8.5	5.3	0.60	2.1
B14		1.7	13.7	1105	129	976	4.4	0.086	11.4	6.6	0.53	2.4
B15	4	4.2	12.1	1100	86	1015	6.1	0.054	17	4	0.82	4.8
B16	3	3.6	10.6	745	102	643	3.8	0.039	13.5	3.8	0.64	4.5
B17		4.1	17.5	1051	118	933	3.8	0.080	26	6.3	0.50	6.0
B18		1.5	12	864	113	751	3.9	0.067	8.3	5.5	0.54	2.1
B19		5.0	11.8	843	60	783	5.8	0.047	25.4	5.1	0.83	5.6
B20		4.8	5.7	631	41	590	6.0	0.020	14.4	3	1.19	4.3
B21		3.4	11.8	1274	48	1227	3.7	0.030	5.3	1.5	0.70	4.2
B22	1	3.8	11.1	625	25	600	5.9	0.026	6.5	1.7	1.06	3.6
B23	3	3.5	5.5	329	34	295	3.9	0.027	9.2	2.7	0.77	4.0
B24	1	6.1	9.3	1253	37	1216	4.6	0.040	11.1	1.8	0.74	7.2
B25	1	7.1	9.2	1162	20	1162	4.1	0.035	8	1.1	0.71	8.5
B26		3.5	12	1175	20	1175	1.6	0.025	7.7	2.2	0.40	5.5
B27	21	4.5	14.7	1175	67	1175	3.2	0.052	18.6	4.1	0.51	6.5
B28		2.2	7.3	526	5	521	3.7	0.053	4.9	2.3	0.56	2.9
B29		3.6	9.7	1195	10	1186	3.2	0.029	5.8	1.6	0.64	4.6
B30	1 (9-B30, B31, B32)	2.1	9	864	59	805	1.7	0.036	6.5	3.1	0.35	3.5
B31	(9-B30, B31, B32)	0.3	7.1	262	92	170	1.6	0.063	1.6	5.4	0.28	0.5
B32	2 (9-B30, B31, B32)	0.2	5.8	281	144	137	1.3	0.079	1.3	7.8	0.21	0.3
B33	(9-B33, B34)	0.1	6.2	261.5	164.5	97	0.4	0.063	0.4	5.6	0.10	0.2
B34	(9-B33, B34)	1.6	10.7	880	172	708	1.6	0.082	3	1.8	0.25	3.1
B35		0.2	7.9	351	191	160	0.6	0.043	0.6	3.3	0.15	0.4
B36		0.7	16.2	592	194.5	397	2.0	0.065	3.6	4.9	0.32	1.2
B37	3	8.2	14.9	1274	46	1228	5.2	0.043	10.7	1.3	0.80	9.7

Table 1. Geomorphological and run-off data for the Somma-Vesuvius basins: number of flood events for single (ne) and multiple, cumulative basins (nep); A (drainage basin area); BMS (Basin Mean Slope); BMe (Basin Maximum elevation); Bme (Basin minimum elevation); BR (Basin relief = BMe minus Bme); La (length of the main stream); S (average slope of the master stream); TL (Total stream length); DD (drainage density); Tc (time of concentration); Qs (Specific discharge rate).

The hypsographic curves analysis highlights the different evolution and maturity of the river basins respectively set up on the three different volcanic sectors (Figure 6). The Mt. Somma river basins of sector A show normal trend with upwards concave hypsographic curves and good index of maturity [Strahler 1957]

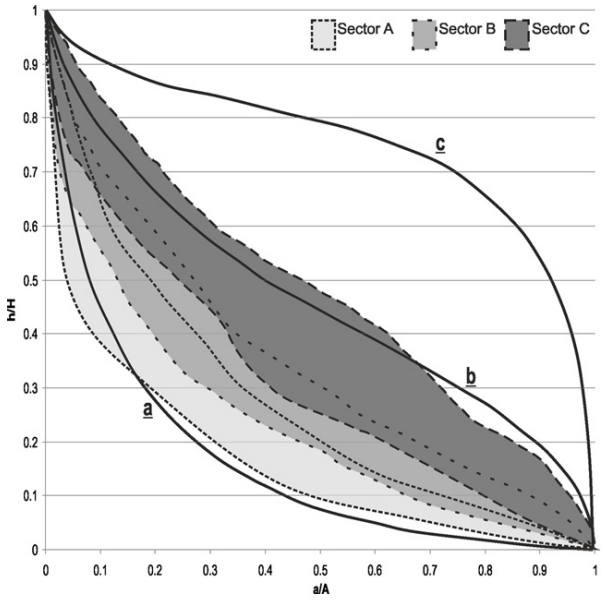

Figure 6. Envelope of the hypsographic curves of the Somma-Vesuvius river basins for the A, B and C sectors and classification according to Strahler [1957]: a = old stage; b = mature stage; c = young stage.

(Figure 6). The hypsographic curves analysis of the Somma-Vesuvius sector B shows on the contrary an irregular trend with many concavity / convexity variations (between mature and old stage). The curves relative to the basins of sector C confirm an upwards concave trend, similar to those of the N sector but with an index of maturity closer to mature stage (line *b* in Figure 6).

The topographical profiles of the basins nos. 15, 24 and 29 clearly show the morphological diversity relative to the three sectors A, B and C (Figure 7). In detail, it is possible to individuate the buried morphological imprint of the Somma caldera old rim (cS), located downhill compared to the base level of Vesuvius cone (bV), with an elevation higher than 800 m a.s.l. (Figure 7).

The drainage network detailed analysis therefore points out the different drainage density of the sectors A and B of the volcanic complex with an average value of about 7 km^{-1} for the Mt. Somma mountainsides (northern) and 3 km^{-1} for the Somma-Vesuvius complex (southern). Thus the sector B drainage network is in general less developed respect to the Mt. Somma sectors, due to its younger topographical surface and results to be strongly controlled by the lavas emplacement due to effusive volcanic activity. Only the no. 26 and no. 27 basins on the southern side of the volcanic complex (see Figure 5 and Table 1) show more developed drainage network because they appear superimposed on a relict surface of the Mt. Somma caldera where mostly loose pyroclastic fall and flow deposits (which are more erodible) are found, besides a few lava flows.

2.3. The database of pluviometric events and historical record of floods

Extensive historical data collection about the local alluvial and landslides events have been carried out through archives and database online on the Web [AVI and IFFI Project], municipal and newspapers libraries, and scientific articles. In our current research 87 flood events have been surveyed (Table 2), but very few landslides retrieved, mostly consisting of small size rock falls, caused by antropogenic activity. There is scarce information about flow-type landslides.

The events have generally occurred just downstream the river basin closures and in areas currently highly urbanized (Figure 5). Among all the other events occurred in the nineteenth century, only for the 1906 May alluvial event, some relationships seem to exist between the event occurrence and the preceding famous 1906 volcanic eruption which began only one month

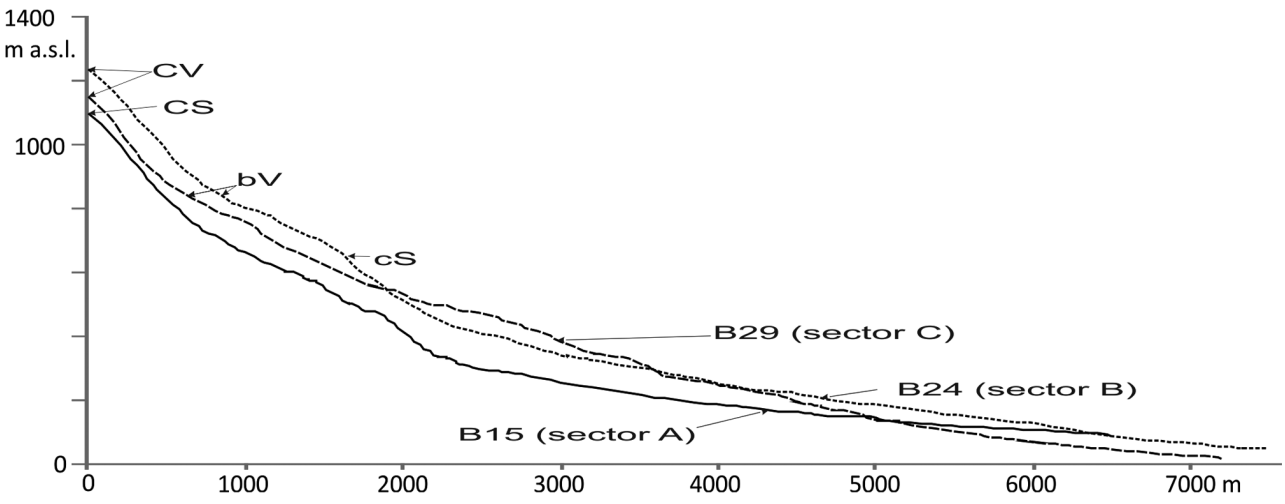

Figure 7. Topographical profiles of the nos. 15, 24 and 29 basins respectively located in the A, B and C sectors of the Somma-Vesuvius volcanic complex CV: active crater of the Vesuvius; CS: rim of the Mt. Somma caldera; cS: buried morphologic rim of Mt. Somma; bV: base level of the Vesuvius cone.

No.	Municipality	Locality	Day	Month	Year	Rainfall duration	Hourly rain (mm)	Daily rain (mm)	Victims	Source
1	Barra		24-25	10	1908		nds	70.2		b,c,d,l
2	Barra		25	10	1921		nda	113.6		c,d,l
3	Boscoreale		21	9	1911		nda	118.9		a
4	Boscoreale	via Diaz	13	11	1997	7 hrs 40 min	39.4	58.2		a
5	Boscotrecase		4	10	1909		nda	9.3		a
6	Boscotrecase		24-25	10	1910		nda	nda		n.
7	Cercola		?	6	1906		nda	15.2		a,c,d
8	Cercola		24-25	10	1910		nda	nda		a,g,n
9	Cercola		30	12	1957	1 hrs 20 min	0.9	1.5	2	a, e, i
10	Cercola		13	11	1997	7 hrs 40 min	39.4	58.2		a
11	Ercolano	-	17 -18	5	1906		nda	11.2	2	a,c,l
12	Ercolano	-	4	1	1907		nda	120		a
13	Ercolano	-	24-25	10	1908		nda	70.2	2	b,c,d,l
14	Ercolano	Resina	24-25	10	1910		nda	nda		n
15	Ercolano	Resina (via Pugliano, via Mare, via Cortile, via Trentola)	21	9	1911		nda	118.9	10	a,g,l
16	Ercolano		25	10	1921		nda	133.6		c,d,l
17	Ercolano		5	11	1954		nda	11		a,e
18	Ercolano		19	9	1960	4 hrs 10 min	57	62.1	1	a
19	Ercolano	via Palmieri	30-31	10	1985	1 hr	43.2	47	1	a,f,g,i,l
20	Ercolano	via Palmieri	2	11	1985		nda	27.2	1	a,l
21	Ercolano		13	11	1997	7 hrs 40 min	39.4	58.2		a
22	Ercolano	via Caprile	27	12	2000	17 hrs	10.0	36.4		a
23	Massa di Somma	via Paparo	22	8	1996	4 hrs	48.4	73.2		a
24	Ottaviano		21	9	1911		nda	118.9		a,g
25	Ottaviano	Cemetery	30-31	10	1985	1 hr	43.2	47		a,
26	Pollena Trocchia			6	1906		nda	15.2		l
27	Pollena Trocchia		24-25	10	1910		nda	nda		n
28	Pollena Trocchia		21	10	2011				1	newspapers
29	Portici		24-25	10	1908		nda	70.2		b,c,d,l
30	Portici		24-25	10	1910		nda	nda		n
31	Portici		21	9	1911		nda	118.9		a
32	Portici		25	10	1921		nda	133.6		c,d,l
33	Portici		19	9	1960	4 hrs 10min	57	62.1		a
34	Portici		1	10	1970	7hrs 20min	17.4	53.2	1	g
35	Portici	Railway	30-31	10	1985	1 hr	43.2	47		i,f
36	Portici		16-17	11	1985	3 hrs	82.4	129		a
37	Portici		18	4	1992		nda	4.4	1	a
38	San Gennaro Vesuviano		30-31	10	1985	1 hr	43.2	47		i
39	San Gennaro Vesuviano		22	8	1996	4 hrs	48.4	73.2		a

No.	Municipality	Locality	Day	Month	Year	Rainfall duration	Hourly rain (mm)	Daily rain (mm)	Victims	Source
40	San Giorgio a Cremano		24-25	10	1908		nda	70.2		b,c,d,l
41	San Giorgio a Cremano		25	10	1921		nda	133.6		c,d,l
42	San Giorgio a Cremano		22	9	1969	19 hrs	3.2	35.9		a,e,h
43	San Giorgio a Cremano	via Tufarelli	16-17	11	1985	3 hrs	82.4	129		i
44	San Giorgio a Cremano	via Matteotti 46	22	8	1996	4 hrs	48.4	73.2		a
45	San Giovanni a Teduccio		24-25	10	1908		nda	70.2		b,c,d,l
46	San Giovanni a Teduccio		24-25	10	1910		nda	nda		n
47	San Giovanni a Teduccio		21	9	1911		nda	118.9		a
48	San Giovanni a Teduccio		25	10	1921		nda	133.6		c,d,l
49	San Giuseppe Vesuviano		21	9	1911		nda	118.9		a,g
50	San Giuseppe Vesuviano		10	1	1956	2 hrs 5 min	3.7	7.3	3	a
51	San Giuseppe Vesuviano		10	1	1997	19 hrs	19	76.8		a
52	San Sebastiano al Vesuvio		24-25	10	1910		nda	nda		n
53	San Sebastiano al Vesuvio		13	11	1997	7 hrs 40 min	39.4	58.2		a,e
54	Sant'Anastasia			6	1906		nda	15.2		a,l
55	Sant'Anastasia		24-25	10	1910		nda	nda		n
56	Sant'Anastasia		13	5	1963	5hrs 4 min	4.2	10.8		a
57	Sant'Anastasia		21	8	1997	2 hrs 50 min	20.0	30.4		a,c
58	Somma Vesuviana		24-25	10	1910		nda	nda		n
59	Somma Vesuviana		26	7	1948	20 min	3.7	3.7		a
60	Somma Vesuviana		14	8	1950	30 min	1.3	1.3		a
61	Somma Vesuviana		2	9	1950	1 hr	13	29.7		a
62	Somma Vesuviana		21	8	1997	2 hrs 50 min	20.0	30.4		a
63	Somma Vesuviana		13	11	1997	7 hrs 40 min	39.4	58.2		a
64	Somma Vesuviana		30	7	2010					a
65	Torre Annunziata		1	10	1970	7hrs 20min	17.4	53.2	1	g
66	Torre del Greco	via XX Settembre, via Cavallerizza, via Purgatorio, Piazza del Popolo			1906				26	c,d,l
67	Torre del Greco		24-25	10	1908		nda	70.2	some	b,c,d,h,l
68	Torre del Greco	via XX Settembre 23	24-25	10	1910		nda	nda	5	h,n
69	Torre del Greco	via XX Settembre, via Nazionale, vico Fiorillo, via Umberto	21	9	1911		nda	118.9	6	d,g,h
70	Torre del Greco		25	10	1921		nda	133.6		c,d,h,l
71	Torre del Greco		7	7	1961	1hr 30 min	9.1	12.8	1	g,h
72	Torre del Greco		12	11	1961	4 hrs 30 min	29	66	2	a,g
73	Torre del Greco		1	10	1970	7hrs 20min	17.4	53.2		g
74	Torre del Greco		19	9	1973		nda	49.6	2	g,l
75	Torre del Greco		13	10	1976		nda	44.2	1	a
76	Torre del Greco*	via Cavallo	29	10	1979		-		2	a
77	Torre del Greco	via Cavallo	19	12	1982		nda	14	2	a,g,l

No.	Municipality	Locality	Day	Month	Year	Rainfall duration	Hourly rain (mm)	Daily rain (mm)	Victims	Source
78	Torre del Greco	via Cavallo	30-31	10	1985	1 hr	43.2	47		a,f,g,i,l
79	Torre del Greco		1	11	1985		nda	54		a
80	Torre del Greco	via Cavallo, via Novesca, via Sant'Elena	16-17	11	1985	3 hrs	82.4	129		f,i
81	Torre del Greco	Piazza Santa Croce	15	7	1991	2 hrs 40min	15.4	16.8		a
82	Torre del Greco	Harbour	26	3	1992	4 hrs 10min	2.4	4.8		a,c
83	Torre del Greco		5	8	1992	40 min	12	12		a
84	Torre del Greco	Piazza Palomba	3_4	10	1992	5hrs 10min	27.8	61.8		c
85	Torre del Greco	Harbour, via XX Settembre	22	8	1996	4 hrs	48.4	73.2		a
86	Torre del Greco	via Beneduce	13	11	1997	7 hrs 40min	39.4	58.2		a
87	Torre del Greco	Santa Maria La Bruna	19	11	2000	12 hrs 30 min	4.8	21.2		a

Table 2 (continued from previous two pages). Main flood events retrieved in this study from 1900 till today relative to each Municipality: a) Catalogo AVI; b) Giangreco e Bonaduce 1999; c) Russo et al. 1995; d) Accardo et al. 1981; e) Vallario 1993; f) Davoli et al. 2001; g) Cosenza 1997; h) Migale and Milone 1998; i) Catenacci 1992; l) Carlino 2001; m) De Vita and Vallario 1996; n) Gazzetta Ufficiale del Regno d'Italia. *For the event no. 76 occurred in 1979 in Torre del Greco the Osservatorio Vesuviano pluviograph had not recorded the rainfall events really abundant according the Capodichino pluviograph record (106 mm). nda = no data available.

before, approximately, therefore showing characteristics similar to a lahar event.

The years with the greatest number of floods were the 1910, 1985 and 1997 with 11, 11 and 10 events, respectively (Figure 8). A significant gap in the years before and after the Second World War has been observed, as well as also a high concentration of events in the first decade of the century, between 1906-1910 (24 events) and between 1990-2000 (21 events), when a considerable urban expansion occurred. Overall, the alluvial events have caused extensive damages and more than 70 casualties.

The space location of floods shows a concentration mainly in the SW, W and NW sectors of Somma-Vesuvius (Figure 5). Few cases have been reported in the NE and SE sectors of the volcanic system. The most hit municipalities have been Torre del Greco (25%), Ercolano (14%) Portici (10%) and Somma Vesuviana (9%), which are located in the N, NW and SW zones of the Somma-Vesuvius; as regards the northern side, a strong concentration of events at Somma Vesuviana has been recorded (Figure 5 and Table 2).

2.3.1. The main historical alluvial events

Historical documents more frequently describe a series of destructive events related mainly to lahar phenomena. Numerous chronicles describe the extensive lahars which affected the volcano during and immediately after its major eruptions (472, 1631, 1707, 1767, 1776, 1794, 1822) with the mobilization of enormous quantities of muddy material that invaded the downstream areas causing extensive damage and many deaths, especially in the towns of Torre del Greco, San Giorgio a Cremano, Ercolano, Portici, Ottaviano, Somma Vesuviana, Pollena-Trocchia, S. Anastasia [Carlino 2001].

In this paper we have studied only the alluvial phenomena *sensu strictu*, ignoring the well-known lahars phenomena, starting from 1906, when a long series of catastrophic hydrogeologic events have occurred, such as the May 17th and 18th events with heavy damages to Ercolano, and the October 25th event, when heavy rainfall (70 mm in a day, recorded at the rain gauge of Ercolano) caused mudslides damaging homes and causing deaths in the areas of San Giovanni a Teduccio, Barra, San Giorgio a Cremano, Portici, Ercolano and Torre del Greco. Two other very destructive floods occurred on October 24th, 1910, with many victims in the countries around the Somma-Vesuvius area, the Amalfi Coast and the island of Ischia; on September 21st and 22nd, 1911, that caused serious damages to the Ercolano town, which was isolated under meters of mud (Figure 9).

In particular, with regard to the 1910 disastrous flood, there is a long record in the Gazzetta Ufficiale del Regno which recounts: "The heavy rainfall occurred in the last night have caused flooding of many houses, making some of them to collapse and causing serious damages [...] Tonight a dead woman was found lying on the street [...] Huge mountain streams of water and mud have fallen from the Vesuvius slopes between

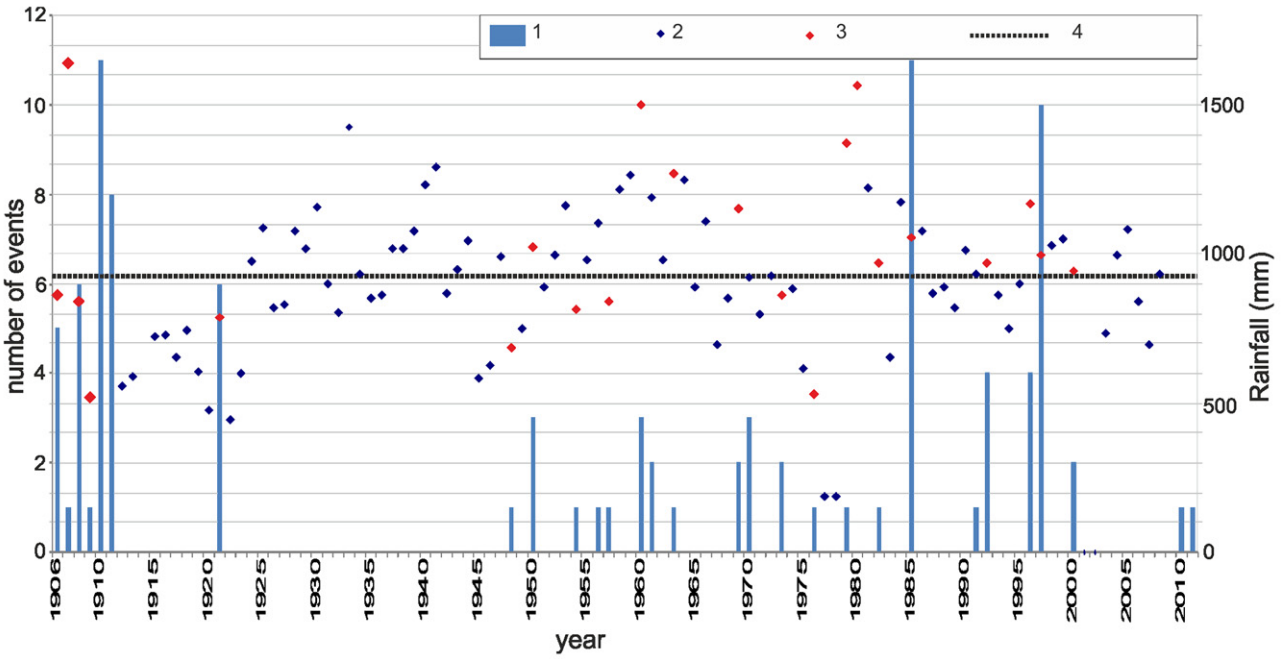

Figure 8. Yearly distribution of the events: 1) number of events; 2) cumulative yearly rainfall; 3) cumulative yearly rainfall relative to the year of the specific event; 4) average value of the yearly rainfall.

Resina and Torre del Greco villages causing heavy damages [...] and have invaded the urbanized areas of Resina and Torre del Greco. In Torre del Greco the street '20th of September' has been almost completely devastated".

Another very intense flood event occurred in October 1921, and affected the inhabitants of Barra, Ercolano, Portici, San Giorgio a Cremano, San Giovanni a Teduccio, Torre del Greco.

Figure 9. Flood event occurred in Ercolano, September 21, 1911 (from Gaudio [1990]).

After a relatively quiet period, other major floods have occurred from 1947 to 2011 [Catenacci 1992]. Among all, the 1969, 1979, 1982, 1985, 1996, 1997, 2000 events have been the most relevant. Torre del Greco and Ercolano towns were the two most damaged localities. In particular, along the street named "Cavallo" at Torre del Greco, several people were killed, drifted to the sea from the alluvial events of the 1969, 1979 and 1982. A similar event has occurred in Ercolano on 1985 and during a storm a man was taken from the water, transported from the water and never found.

Summarizing the above, it can be said that the Torre del Greco and Ercolano towns, the southern side of Portici and the northern side of Somma Vesuviana have been the areas with higher occurrence of alluvial catastrophic events. In the last century these areas were affected 8 to 25 times by floods, with very low return periods, therefore approximately once every ten years (Table 2).

2.3.2. Hydrological trends

During the whole period of occurrence of the main flood events, yearly rainfall values larger of the average value calculated through the Osservatorio Vesuviano pluviometric station, over a time extent of 100 years, have been observed (Figure 10). The flood events have occurred all over the year (Figure 10a), with a concentration significantly greater during October (35%). Accordingly, the average monthly rainfall diagram (computed over 100 years) shows the typical trend of temperate climate with a maximum value recorded in November. The monthly rainfall curve shows a strong rise from September to November,

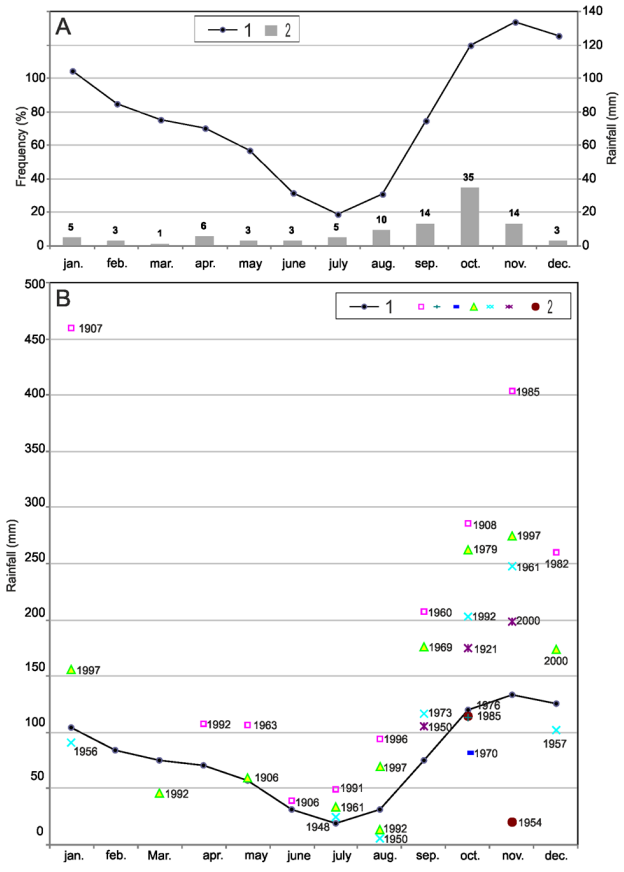

Figure 10. Flood events and monthly rainfall. A) relationship between the the monthly average rainfall curve since 1906 (1) and frequency of the events (2); B) correlation between the monthly rainfall observed for all events and the monthly average rainfall curve; 1) monthly average rainfall curve; 2) cumulative monthly rainfall for each event.

when a percentage of about 62% of events are observed (Figure 10a). The monthly average rainfall values at the Osservatorio Vesuviano pluviometric station are almost always overcome by real rainfall occurred during the flood events activation periods (Figure 10b).

Rainfall qualitative description	Relative daily rainfall quantity
Light	<20 mm
Moderate	20-60 mm
Heavy	60-100 mm
Very heavy	>100 mm

Table 3. Rainfall qualitative description versus the corresponding daily rainfall quantity.

The rainfall intensity calculated, whenever possible, for some events (44 events), has been associated to strong but not violent rainfall events (Figure 11a), since the critical value of 50 mm/h (violent rain) has never been overcome [Glossary of Meteorology 2000]. As regards the flood phenomena, for each flood event the daily and hourly pluviometric data have been collected; particularly, analyzing the *Bollettino di Vigilanza Meteorologica Nazionale* of the Civil Protection National Department which gives a classification of the daily rainfall (Table 3), only for 27% of cases very large rainfall phenomena are pointed out (Figure 11b).

With regard to the relationship between the rainfall and the flood events, at least in the last century the rainfall events have been mostly concentrated over the southern sector of Somma-Vesuvius, the hourly precipitations have not been extraordinary, the return periods could be therefore of ten years.

For each basin the time of concentration (tc) was calculated by means of the Kirpich formula [Kirpich 1940] that can be applied to basins of limited size and utilized by Santo et al. [2012] for similar geologic contexts (Table 1):

$$tc = 0.000325\ (L/ia)^{0.77}$$

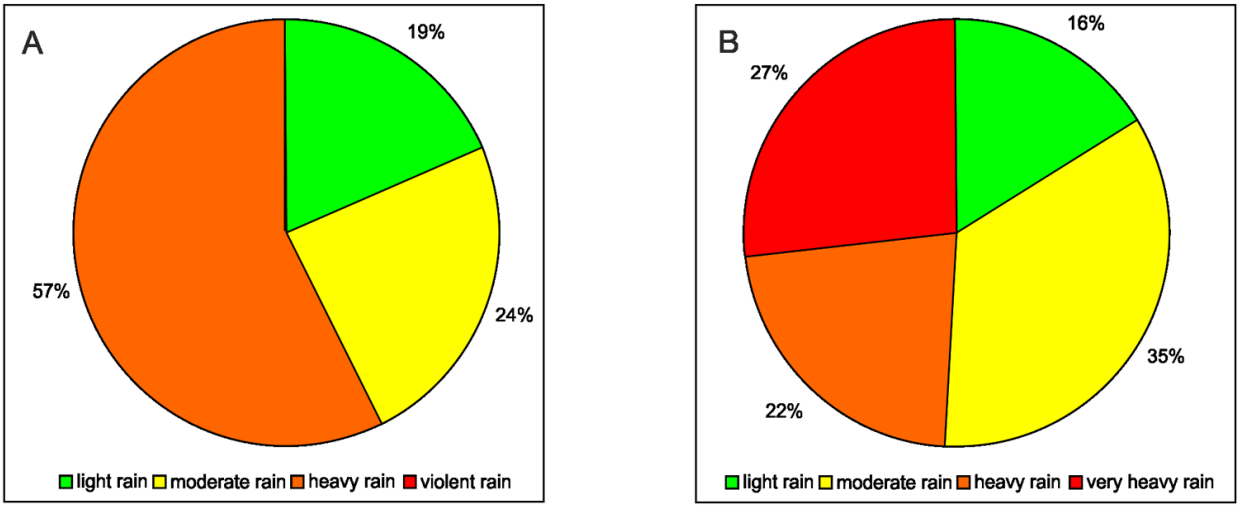

Figure 11. Daily rainfall classification of the counted flood events: A) from Glossary of Meteorology [2000]; B) from *Bollettino di Vigilanza Meteorologica Nazionale* of the Civil Protection National Department.

where time of concentration (*tc*) is expressed in hours, *L* (in meters) is the length of the main stream calculated from the watershed, and *ia* is its gradient (m/m) estimated by means of Taylor and Schwartz [1952] formula.

In order to estimate the index peak discharge of each basin we applied the well-known rational formula [Rossi and Villani 1995]:

$$\mu_c = \frac{C\mu[h(t_c)]A}{3.6} \qquad (2)$$

where: A is the catchment area of the basins; C is the runoff coefficient; $\mu[h(t_c)]$ is the mean of annual maximum rainfall depth within a time interval equal to the catchment concentration time, t_c, estimated from the regional rainfall height duration curve at the mean catchment elevation.

The runoff coefficient is assumed equal to 0.13, as suggested by the regional flood frequency procedure for similar catchments. The catchment concentration times (Table 1) are considered the critical duration of the rainfall for the maximum catchment discharge, according to a kinematic modeling of the catchment response [Chirico et al. 2003, 2005]. Thus, by applying Equation (2), the index flood μQ for the Somma-Vesuvius basins are estimated (Table 1).

2.4. The database of whole infrastructures including changes throughout the last century

During the last centuries the piedmont sector of the Somma-Vesuvius district, as also described in the above paragraphs, has been hit by many alluvial events causing many casualties (more than 70) and heavy damages. Due to these events, on early 17th century, important hydraulic engineering works were created, the "Regi Lagni" channels, inside which the main rivers from the Somma-Vesuvius mountainsides and the nearby calcareous reliefs have joined. Particularly, on early 1900 the "Lagni" of the Somma piedmont zones were built; successively, only in the 1950's, after repeated destructive alluvial events, such works were constructed also on the Vesuvius sector. Due to both the huge population increase of the last 60 years and decreasing frequency of catastrophic events (both of volcanic and alluvial origin), a strong variation of the piedmont sectors hydrographic setting has been induced, which in turn has seriously increased the risk level. By means of topographical maps realized on different epochs and reciprocally compared, the time evolution of the urbanization increase as well as of the hydrographical network for the Somma-Vesuvius district have been evaluated in this paper creating the database of whole infrastructures (examples in Figures 12, 13). The topographical

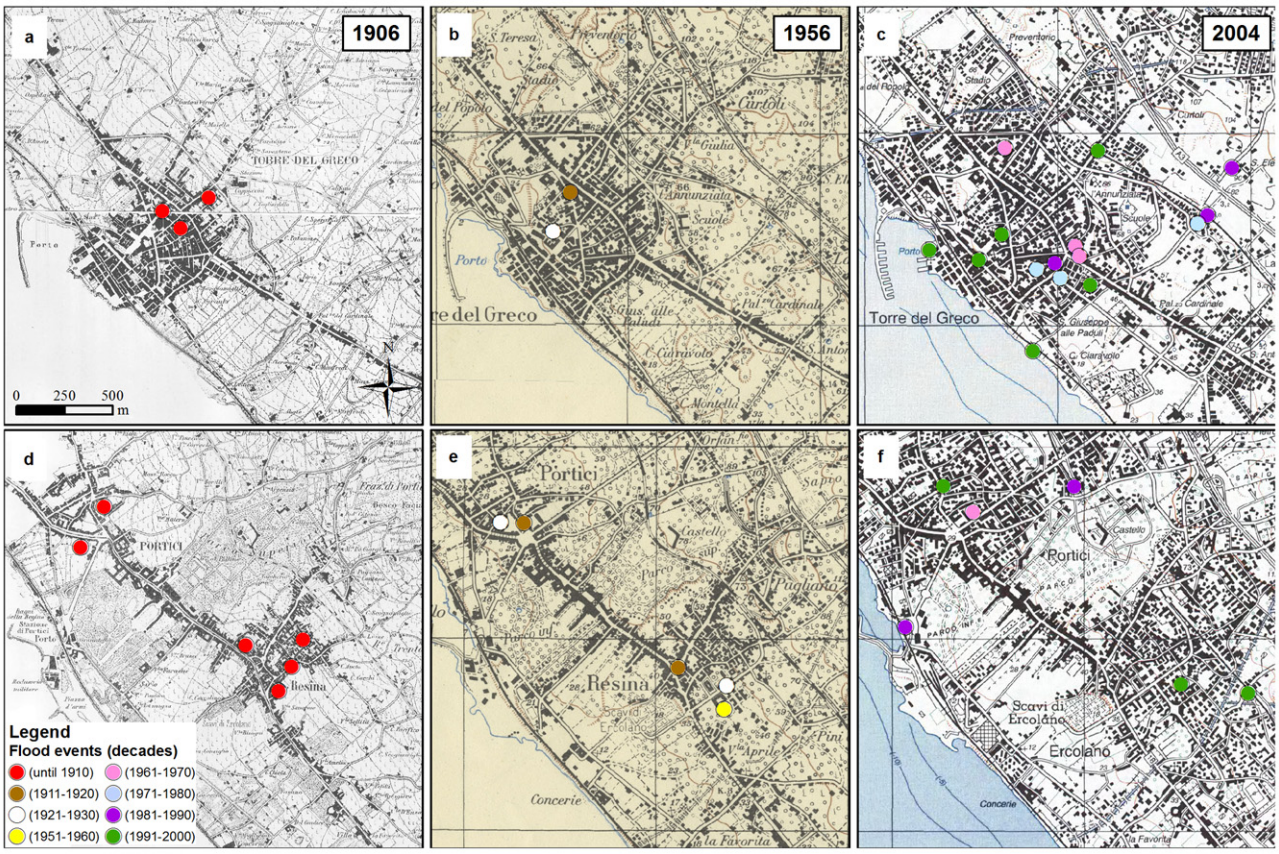

Figure 12. Urbanization variations in the last 100 years; the dots indicate the flood events for different decades; it is evident that many inundations events have hit areas not urbanized at the beginning of the century for Torre del Greco (a,b,c), Portici and Ercolano (d,e,f).

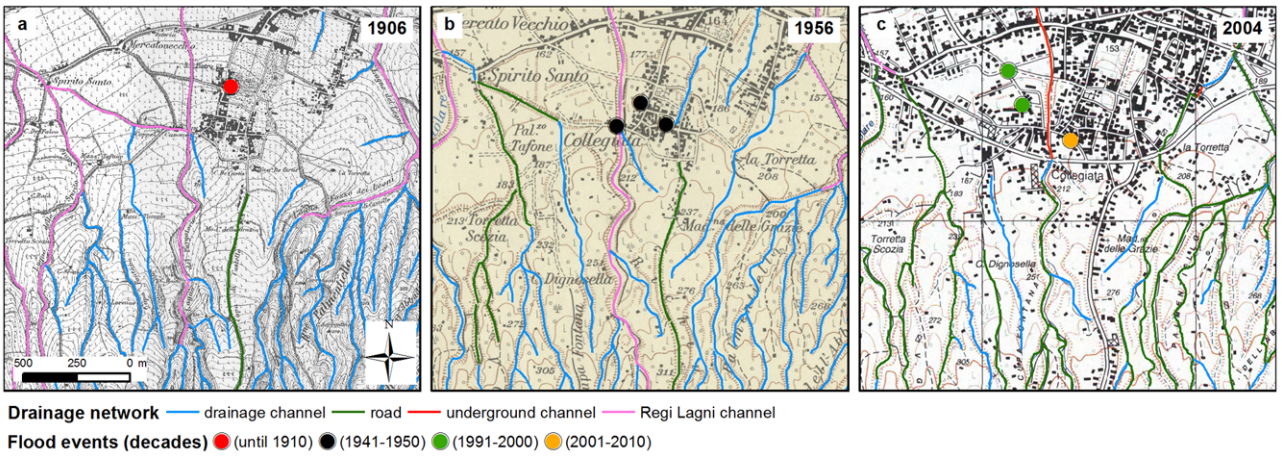

Figure 13. Hydrographical network modifications in 1906, 1956 and 2004 in the Pollena-Trocchia area. The drainage channel is in light-blue colour, the road is in dark-green, the underground channel in red and the "Regi Lagni" channels in magenta.

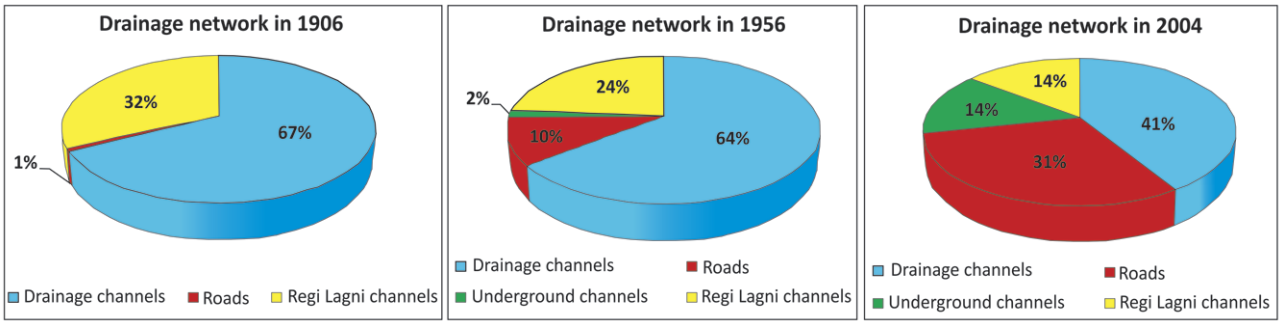

Figure 14. Hydrographical network modifications from 1906 to 2004 for the study area.

maps of 1906 [IGMI - Topographic Map of Mount Vesuvius, 1:10000], 1956 [IGMI - Topographic Map of Italy, 1:25000] and 2004 years [CTR - Regional Technical Map of Campania region 1:5000] have been taken into account and the whole hydrographical network and urbanized areas have been digitized. Particularly, it has been pointed out that from 1906 till today the hydrographical network has been modified by intense urbanization, with many roads being built and the consequent transformation of the natural channels into road-channels or underground channels (Figures 13, 14). In Figure 13 the Pollena Trocchia area is shown, where the natural riverbeds have been converted into roads while some "Lagni" sectors have been tombed. In 1906 the study area was characterized by natural riverbeds (67% of the total length of the hydrographical network) along the mountainsides of the Somma-Vesuvius and in the "Regi Lagni" piedmont areas (32% of the total length of the hydrographical network). Only in few cases some dirt roads and muletracks existed at the outlet of some valleys. In the 1950's a greater urbanization took place, consequently while the "Lagni" were constructed in the Vesuvius sector, between the built-up areas of Ercolano, Torre del Greco and Torre Annunziata, many more roads were

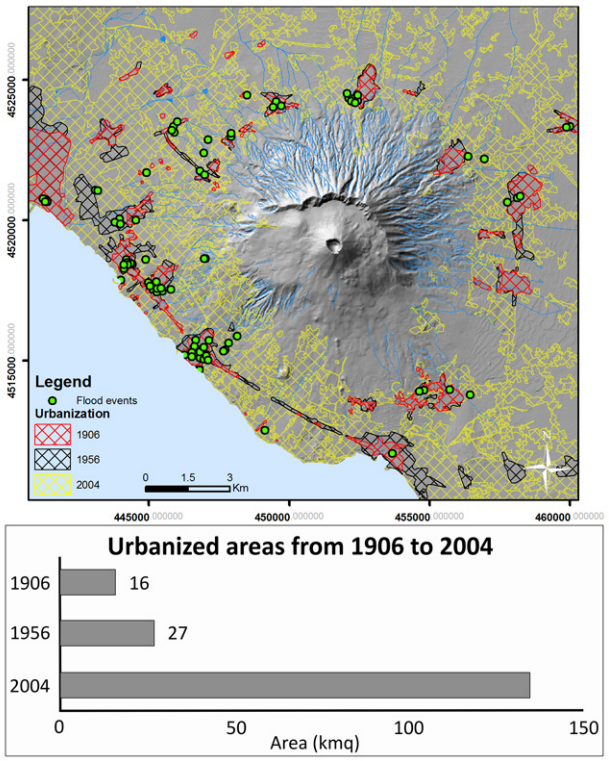

Figure 15. Time evolution of the urbanized areas of the Somma-Vesuvius district from 1906 to 2004.

constructed with the consequence of the "Lagni"'s real detriment or the natural riverbeds detriment (10% of road-channels and 2% of underground channels respect to the total network length) (Figure 14). In the last 60 years, with a greater urbanistic expansion both along the coastal sectors and along the higher sectors of Vesuvius, a big growth of the streets system has taken place with the consequent transformation of the old fluvial riverbeds or the "Lagni" into road-channels (14% of the total length of the hydrographical network) or underground channels (31% of the total length of the hydrographical network) (Figure 14). Synthetically, it is possible to confirm that, from 1906 till today, the natural riverbeds percentage has decreased of 20%, while the road-channels and underground channels percentage has increased to 30% and 15%. Therefore, starting from an area of 16 km^2 in 1906, it has become of 27 km^2 in 1956, and 135 km^2 in 2004 (Figure 15). Actually, in the last 60 years the urbanization expansion has been much greater than that of the previous 60 years, with a percentage increase of 70 % from 1906 to 1956 and of 400% from 1956 to 2004, also due to a quiescence state of the Vesuvius eruptive activity, which last eruption dates back to 1944 (Figure 15).

In conclusion, during the last century a huge expansion of the urbanized areas has taken place; this situation, besides increasing the risk level due to the increase of the exposed value, has also massively modified the natural course of the riverbeds which have been transformed into road-channels or underground channels.

3. Results and conclusions

In this paper historical chronicles on flood events and hydrological data have been investigated together with geomorphological and geological parameters for characterizing the susceptibility of the Somma-Vesuvius volcanic district to flood events.

Historical analyses show that since 1900 the southern sectors of Mt. Vesuvius (towns of Torre del Greco, Ercolano and Portici) and the northern sector of Mt. Somma (particularly Somma Vesuviana town) have been the areas mostly affected by destructive floods.

The main results have also evidenced that the most frequent geomorphologic set up is typical of torrential basins with high slope and high relief energy, such basins being active only during intense rainfall events. During these events the streams become able of trans-

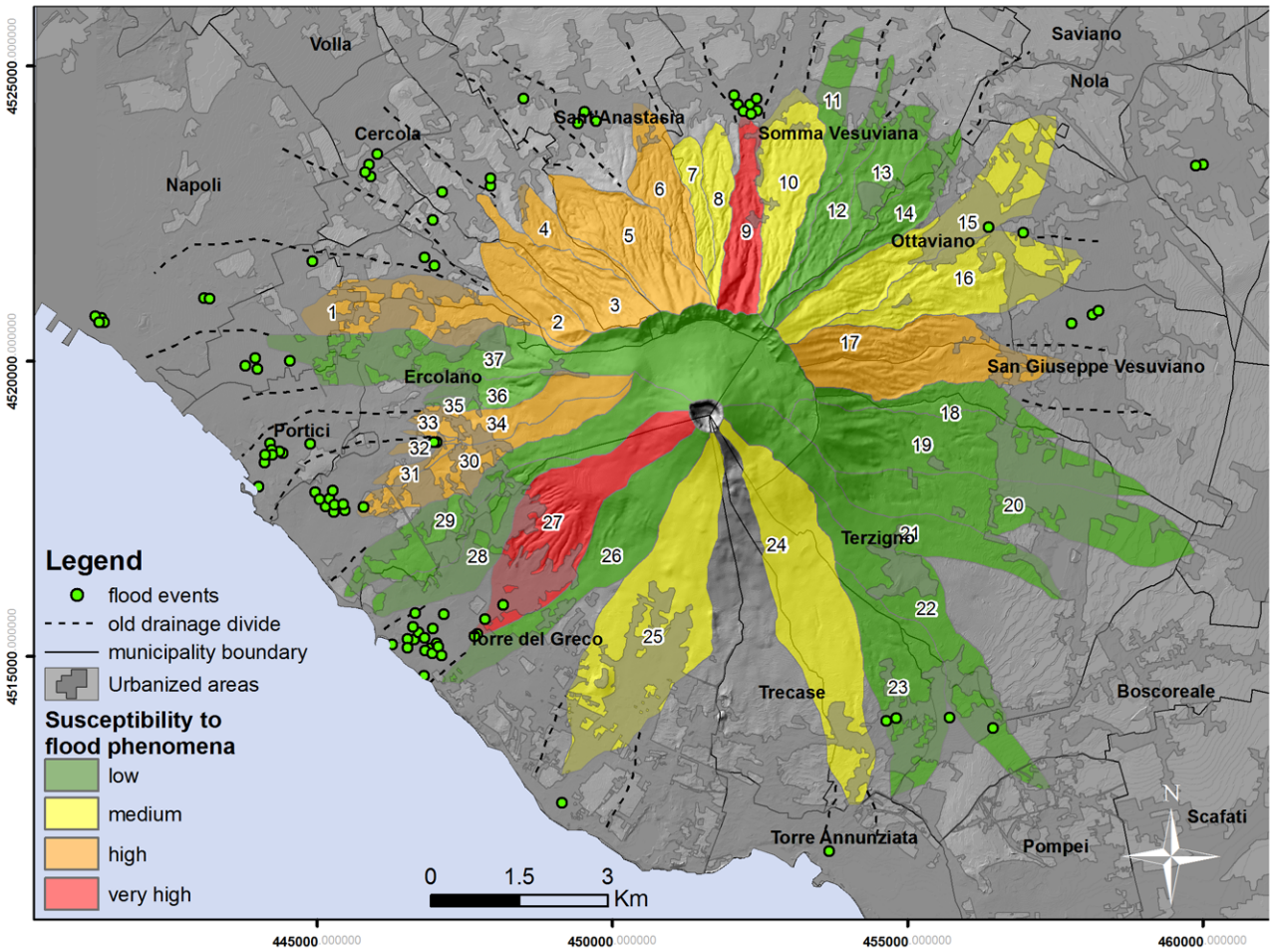

Figure 16. Preliminary zoning of the susceptibility of the Somma-Vesuvius district to flood phenomena.

porting large quantities of solid material downstream, especially in those basins with larger thickness of loose pyroclastic products.

The floods are correlated with heavy, but not extraordinary, daily rainfall (<50 mm/day), especially when the hourly intensity is high. It might be hypothesized that larger rainfall values observed on the southern slopes have also been caused by the prevailing winds regime blowing from SW to NE.

The considerable observed damages are due to the heavy urbanization in the piedmont areas, to the local geomorphological conditions of the Somma-Vesuvius, and to human actions on the catchment areas, often transformed into channel-roads or tapped-channels over very long stretches of the roads themselves. The damages reported in the historical chronicles were considerable although the urbanization was very different from the current one; the intense urban expansion of the last years (after 1950) has highlighted an even higher risk level for this area.

By means of a GIS application the different parameters before mentioned (drainage density, time of concentration, specific discharge and amount of events) have been qualitatively analyzed for drafting a preliminary susceptibility map of the whole area to the flood phenomena, where the flood events recorded at the beginning of 1900 have been located according to the coeval urban structure (Figure 16). In order to obtain the susceptibility classes, the above parameters have been classified in three classes (low, medium, high) by assigning to each of them the values 1 to 3. Such values have been successively summed up and the final susceptibility values have been obtained coming out in four classes (low, medium, high and very high). The maximum susceptibility is shown by the basins no. 27 and no. 9. In general, the minimum susceptibility is observed for the southeastern basins, whereas the maximum values are found for the northwestern and southwestern basins; therefore in Figure 16 the basins where most probably floods could originate are pointed out, together with the densely urbanized areas down to the plain, possibly exposed to such floods in the future.

In conclusion our analysis has shown that the Somma-Vesuvius volcanic district, well known to the scientific community and Institutions for its very high volcanic risk, also show evidences of high floods hazard. Most of the floods retrieved from historical chronicles have affected the western and southwestern municipalities of the area, particularly Torre del Greco, Ercolano, Portici e Somma Vesuviana, with recurrence times of ten years approximately. The data collected in this study have allowed us to work out a preliminary and qualitative susceptibility map, while a more detailed and rigorous analysis will be the subject of future work. Particularly for the basins with higher susceptibility values, it would be appropriate to carry out more detailed studies based on hydraulic parameters, through semi-empirical and physical methods, and taking into account an accurate geomorphological model and the distribution and typology of the existing antropogenic manufactures. Such studies could be included in the Civil Protection early warning plains for floods hazard, as well as interventions useful for mitigation of hydraulic risk should be implemented in the next future.

References

Accardo, A., P. Bianucci, V. Bonaria and S. Gaglione (1981). Il bacino imbrifero del Vesuvio: dissesti idrogeologici e difesa del territorio. Conv. Interclubs Rotary Club - Lyons Club, Torre del Greco, 13 pp.

Andronico, D., R. Cioni, P. Marianelli, R. Santacroce, A. Sbrana and R. Sulpizio (1996a). Introduction to Somma-Vesuvius, In: Vesuvius Decade Volcano, Workshop Handbook (Naples, September 17-22, 1996).

Andronico, D., R. Cioni and R. Sulpizio, (1996b). General stratigraphy of the past 19,000 yrs at Somma-Vesuvius, In: Vesuvius Decade Volcano, Workshop Handbook (Naples, September 17-22, 1996).

Andronico, D., and R. Cioni (2002). Contrasting styles of Mount Vesuvius activity in the period between the Avellino and Pompeii Plinian eruptions, and some implications for assessment of future hazards, Bull. Volcanol., 64, 372-391.

AVI Project. Catalogo nazionale delle località colpite da frane e da inondazioni. Gruppo Nazionale per la Difesa dalle Catastrofi Idrogeologiche; http://avi.gndci.cnr.it/.

Carlino, S. (2001). Le alluvioni e le colate di fango successive alle eruzioni. Storia e considerazioni sul rischio, In: C. Bifulco (ed.), Interventi di ingegneria naturalistica nel Parco Nazionale del Vesuvio, Ente Parco Nazionale del Vesuvio, San Sebastiano al Vesuvio (Napoli), 43-69.

Catenacci, V. (1992). Il dissesto idrogeologico e geoambientale in Italia dal dopoguerra al 1990, Serv. Geol. Naz. - Memorie Descrittive della Carta Geologica d'Italia, 47, 1-301.

Chirico, G.B., R.B. Grayson and A.W. Western (2003). On the computation of the quasidynamic wetness index with multiple-flow-direction algorithms, Water Res. Res., 39 (5), no. 1115.

Chirico, G.B., A.W. Western, R.B. Grayson and G. Blöschl (2005). On the definition of the flow width for calculating specific catchment area patterns from gridded elevation data, Hydrol. Process. 19, 2539-2556.

Chirico, A., R. Nappi and G. Alessio (2010). Vulnerabilità del territorio vesuviano a fenomeni meteorologici attraverso l'analisi quantitativa di fattori geologici ed antropici, Poster GIT - Geology and Information Technology, 5ª Riunione del Gruppo di Geologia Informatica - Sezione della Società Geologica Italiana, Grottaminarda (Avellino), 14-16 giugno 2010.

Cioni, R., R. Santacroce and A. Sbrana (1999). Pyroclastic deposits as a guide for reconstructing the multistage evolution of the Somma-Vesuvius caldera, Bull. Volcanol. 60, 207-222.

Cioni, R., A. Bertagnini, R. Santacroce and D. Andronico (2008). Explosive activity and eruption scenarios at Somma-Vesuvius (Italy): Towards a new classification scheme, Journal of Volcanology and Geothermal Research, 178, 331-346.

Cosenza, G. (1997). Area Vesuviana: metastasi di un territorio, In: F. Fiorentino (ed.), Mons Vesuvius, sfide e catastrofi tra paura e scienza, Napoli.

Cotton, C.A. (1944). Volcanoes as landscape forms, Whitcombe and Tombs, Christchurch, N.Z., 416 pp.

CTR - Regione Campania (2004). Carta tecnica regionale, Regione Campania (scala 1:5000).

Davies, T., and M. Mc Saveney (2011) Bedload sediment flux and flood risk management in New Zealand, Journal of Hydrology (NZ), 50 (1), 181-190.

Davoli, L., P. Fredi, F. Russo and A. Troccoli (2001). Natural and anthropogenic factors of flood hazards in the Somma-Vesuvius area (Italy) / Rôle des facteurs naturels et anthropiques sur les risques d'inondation autour du Vésuve-Somma (Italie), In: Géomorphologie: relief, processus, environnement, 7 (3) 195-207.

De Vita, P., and A. Vallario (1996). Il rischio idrogeologico del Somma-Vesuvio, Mem. Soc. Geol. It., 51, 1075-1085.

Di Crescenzo, G., M. De Falco, V.E. Iervolino, S. Rinaldi, N. Santangelo and A. Santo (2008). Proposal of a new semiquantitative methodology for flowslides triggering susceptibility assessment in the carbonate slope contexts of Campania (Southern Italy), Ital. J. of Engin. Geol. and Environ., 1, 61-79.

Gaudio, M. (1990). Ercolano e il Vesuvio - Luoghi, tradizioni, vicende, Comune di Ercolano, Assessorato ai beni culturali.

Gazzetta del Regno d'Italia. Progetto Au.G.U.Sto. (Automazione della Gazzetta Ufficiale Storica); http://augusto.digitpa.gov.it.

Giangreco, E., and G. Bonaduce (1999). Il rischio Vesuvio, Edited by Elio Giangreco, Fridericiana editrice universitaria: Edizioni Scientifiche Italiane, Napoli, 334 pp.

Glossary of Meteorology (2000). Glickman Todd S. American Meteorological Society, 2nd edition.

IFFI Project (Inventario dei Fenomeni Franosi in Italia) ISPRA - Dipartimento Difesa del Suolo-Servizio Geologico d'Italia – Regione Campania (2006): www.sinanet.isprambiente.it/progettoiffi.

IGMI. Carta topografica del monte Vesuvio, (scala 1:10000). Stampa del 1908, colle ricognizioni parziali 1904-1906. Istituto Geografico Militare, Firenze.

IGMI. Carta topografica d'Italia, (scala 1:25000). Serie 25V. Istituto Geografico Militare, Firenze.

Jenness, J., and S. Tagil (2008). Gis-Based Automated Landform Classification and Topographic, Landcover and Geologic Attributes of Landforms Around the Yazoren Polje, Turkey, Journal of Applied Sciences, 8 (6), 910-921.

Karatson, D., T. Telbisz and B.S. Singer (2010). Late-stage volcano geomorphic evolution of the Pleistocene San Francisco Mountain, Arizona (USA), based on high-resolution DEM analysis and Ar-40/Ar-39 chronology, Bull. Volcanol. 72, 833-846.

Kirpich, Z.P. (1940). Time of concentration of small agricultural watersheds. Civil Engineering 10 (6), 362 pp.

Lirer, L., A. Vinci, I. Alberico, T. Gifuni, F. Bellucci, P. Petrosino and R. Tinterri (2001). Occurrence of intereruption debris flow and hyperconcentrated flood-flow deposits on Vesuvio volcano, Italy, Sedimentary Geology, 139, 151-167.

Mastrolorenzo, G., and L. Pappalardo (2010). Hazard assessment of explosive volcanism at Somma-Vesuvius, J. Geophys. Res., 115, B12212, 1-19.

Migale, L.S., and A. Milone (1998). Mud flows in pyroclastic of the Campania. First data from historical research, Rassegna Storica Salernitana, 30, 15 (2), 235-271.

Nappi, R., G. Alessio, G. Bronzino, C. Terranova and G. Vilardo (2008). Contribution of the SISCam Web-based GIS to the seismotectonic study of Campania (Southern Apennines): an example of application to the Sannio-area, Natural Hazards, 45, 73-85.

Nazzaro, A. (2001). Il Vesuvio: Storia eruttiva e teorie vulcanologiche, Liguori Ed., Napoli, 368 pp.

Ollier, C. (1991). Ancient Landforms, Belhaven Press, London/New York, 230 pp.

Pareschi, M.T., L. Cavarra, M. Favalli, F. Giannini and A. Meriggi (2000). GIS and volcanic risk management, Nat. Hazards, 21, 361-379.

Rossi, F., and P. Villani (1995). Flood evaluation in Campania Region (in Italian), Department of Civil Engineering, University of Salerno, GNDCI-CNR, Pubbl. N.1470, 1995.

Russo, F., M. Valletta e C. Granata (1995). Il rischio geologico *in sensu lato* al Somma-Vesuvio, Rend. Acc. Sc. Fis. Mat. - Napoli, 62, 125-186.

Santacroce, R., ed. (1987). Somma-Vesuvius, Quaderni de "La Ricerca Scientifica", CNR, 114, 251 pp.

Santacroce, R., and A. Sbrana (2003). Carta Geologica del Vesuvio - Scala 1.15.000, Progetto CARG, Carta Geologica d'Italia, S.EL.CA., Firenze.

Santo, A., G. Di Crescenzo, S. Del Prete and L. Di Iorio (2012). The Ischia island flash flood of November 2009 (Italy): Phenomenon analysis and flood hazard, Physics and Chemistry of the Earth, 49, 3-17.

Scandone, R., F. Bellucci, L. Lirer and G. Rolandi (1991). The structure of the Campanian plain and the activity of the neapolitan volcanoes, J. Volcanol. Geoth. Res., 48 (1-2), 1-3.

Scandone, R., L. Giacomelli and P. Gasparini (1993). Mount Vesuvius: 2000 years of volcanological observations, J. Volcanol. Geoth. Res., 58 (1-4), 5-25.

Schumm, S.A. (1977). Bench Mark Papers in Geology Ed., vol. 1.

Smith, G.A., and D.R. Lowe (1991). Lahars: Volcano-hydrologic events and deposition in the Debris Flow - Hyperconcentrated flow continuum, In: R.V. Fisher and G.A. Smith (eds.), Sedimentation in Volcanic Settings, SEPM Spec. Publ., 59, 59-70.

Strahler, A.N. (1957). Quantitative analysis of watershed geomorphology, Trans. Amer. Geophys. Union, 8 (6), 913-920.

Taylor, A.B, and H. E. Schwarz (1952). Unit hydrograph lag and peak flow to basin characteristic, Trans. Amer. Geophys. Union, 33, 235-246.

Vallario, A. (1993). Il dissesto idrogeologico in Campania, Ed. CUEN, 304 pp.

Ventura, G., G. Vilardo, G. Bronzino, R. Gabriele, R. Nappi and C. Terranova (2005). Geomorphological map of the Somma-Vesuvius volcanic complex (Italy), Journal of Maps, 30-37.

Vilardo, G, G. Bronzino, G. Alessio, E. Bellucci Sessa and R. Nappi (2008). GeoDATA Finder: Sistema di consultazione on-line della banca dati territoriali del Laboratorio di Geomatica e Cartografia, Istituto Nazionale di Geofisica e Vulcanologia, Sezione di Napoli Osservatorio Vesuviano; http://ipf.ov.ingv.it/dbnas/login_user.asp.

*Corresponding author: Giuliana Alessio,
Istituto Nazionale di Geofisica e Vulcanologia, Sezione di Napoli, Osservatorio Vesuviano, Naples, Italy;
email: giuliana.alessio@ov.ingv.it.